

BUBBLE CHAMBER FILM ANALYSIS

ABSTRACT

The real fundamental physics events in which K^- mesons (1.5 GeV/c) incident on hydrogen nuclei (protons) has been studied with the 70mm film of the hydrogen bubble chambers operating at the Berkeley Bevatron in the 1960's. These events were carefully scanned to determine the K^- life time τ , and the elastic and total cross section areas $\sigma_{el.}$ and σ_{total} respectively. Then I obtained $\tau = (1.04 \pm 0.05)E-8 \text{ sec}$, $\sigma_{el.} = (0.82 \pm 0.04)E-30 \text{ m}^2$, and $\sigma_{total} = (3.51 \pm 0.16)E-30 \text{ m}^2$. Also, based on the measured total cross section, I approximately calculated the proton's effective radius, $R_p = (5.89 \pm 0.14)E-16 \text{ m}$. Moreover, I classified about ten different kinds of interest events found from the film.

THEORY

The most straightforward way to understand the events with the incident K^- beam into the liquid hydrogen bubble chamber is to divide the events into the categories of decays and interactions.

Since the rate of decay with respect to the K^- path length x is proportional to the number of incident beam N and the inversely proportional to the distance K^- travels in its life time τ ,

$$\begin{aligned} \frac{dN}{dx} &= -\frac{1}{v(\gamma\tau)} N & \text{where } \gamma\tau \text{ is the relativistic time.} \\ &= -\frac{1}{\beta\gamma c\tau} N \\ \int \frac{dN}{N} &= -\int \frac{1}{\beta\gamma c\tau} dx & \therefore N = N_0 \exp\left(-\frac{x}{\beta\gamma c\tau}\right) \end{aligned}$$

This is the equation which I use to calculate the K^- life time later on.

Similarly, the rate of interaction with respect to the K^- path length is proportional to the number of incident K^- beam N and the cross section area in unit volume. Since the number of proton in unit volume is $N_a \rho / A$, where N_a is the Avogadro's number, ρ is the density of proton in liquid hydrogen (0.0625 g/cm^3), and A is the atomic weight of proton (1.0069 g/mole), the cross section in unit volume is simply $\sigma N_a / A$.

Then I set

$$\frac{dN}{dx} = -\frac{\sigma N_a \rho}{A} N$$

Similar to the derivation before,

$$N = N_0 \exp\left(-\frac{\sigma N_a \rho x}{A}\right)$$

This is the equation I will use to calculate the cross section of the interaction.

If I combine these two equations above, I will get the new equation expressing the attenuation of beams as a function of the path length x .

$$N = N_0 \exp\left(\frac{-x}{\delta \beta c \tau}\right) \exp\left(\frac{-x N_A \rho \sigma}{A}\right)$$

However, to obtain the life time τ and the cross section σ easily, I assume that the average K^- path length within the fiducial volume, Δx , is still short enough to approximate:

$$\frac{dN_D}{dx} = \frac{\Delta N_D}{\Delta x} \quad \text{and} \quad \frac{dN_I}{dx} = \frac{\Delta N_I}{\Delta x}$$

where ΔN_D and ΔN_I are the numbers of all decays and interactions observed.

On the other hand, since decays in flight remove K^- from the sample that could possibly interact, and vice versa, the number N can be modified to $N = N_0 - (\Delta N_I + \Delta N_D)/2$. (See Appendix 1).

Thus, I obtain:

$$\frac{\Delta N_D}{\Delta x} = \frac{1}{\delta \beta c \tau} \left(N_0 - \frac{\Delta N_I + \Delta N_D}{2} \right) \quad \text{----- (1)}$$

and

$$\frac{\Delta N_I}{\Delta x} = \frac{N_A \rho \sigma}{A} \left(N_0 - \frac{\Delta N_I + \Delta N_D}{2} \right) \quad \text{----- (2)}$$

More accurate calculations for τ and σ is roughly introduced in the Appendix 2.

When we try to understand these events from the respect of the conservation laws, in addition to the familiar laws of conservation of energy, charge, linear and angular momentum, there are the conservation of baryon number, lepton number, and ~~muon family number~~. Also, in hadronic interaction, like K^-p interaction, isospin and strangeness numbers are also conserved. I listed ten different kinds of interesting events found with some of these laws in the Appendix 3.

APPARATUS AND PROCEDURE

At this point, it is appropriate to begin discussing the brief description of the method of producing bubble chamber film and also the scanning machine I used in this experiment.

The first step in the production of bubble chamber picture is the Bevatron (Figure 1), which is a large and complex device. The positively charged protons are injected into the Bevatron with an energy of particular electron volts such as 10MeV.

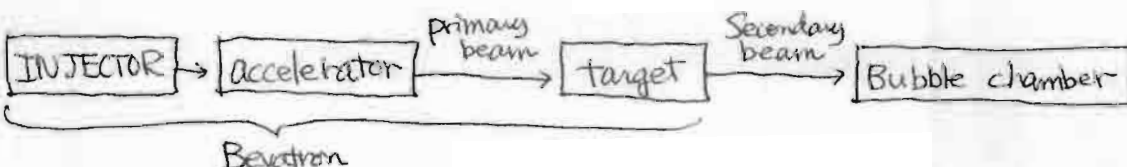


Figure 1

Then the protons are accelerated circularly until they have reached the energy desired by the experimenter. When the accelerating voltage is turned off, the protons gradually spiral inward and strike the target. (Figure 2) Then, an array of particles of all types at a spectrum

of energies are produced. This is the secondary beam. To select the desired momentum is accomplished by a machine called a bending magnet. In order to separate one type of particle from others, a velocity spectrometer is employed. Then the beam is focused with a device called quadrupole magnet.

By combining these devices, K^- meson beam is created and aimed into the bubble chamber.

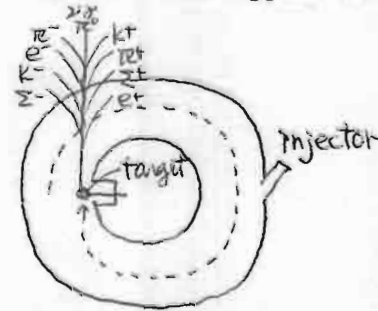


Figure 2

The 25 inch bubble chamber consists of a closed vessel containing a liquid hydrogen with its density approximately 0.06gm/cm^3 at a temperature above its normal boiling point but under a sufficient pressure to prevent boiling. The pressure of the liquid is suddenly released. For a fraction of a second, the liquid hydrogen does not boil but in a superheated state. During this brief moment, the incident beam is fired into the chamber. In a superheated liquid hydrogen, boiling will start with the formation of gas bubbles at nucleation centers in the liquid, and particularly along trails of ions left by the passage of a charged particle. At this point, a photo is taken of the particle tracks. The bubble then collapse under a recompression stroke, and the cycle can be repeated.

Actually, my job is from here. I scanned the events in 500 films taken at the Berkeley Bevatron in 1968. Operation of the film scanning machine SP-V(A) is very simple.

The first step is to turn on the three pole black circuit breaker and push the start button located at the back of the SP-V(A). Then I loaded the film. With the forward/backward controls on the SP-V(A) operator film controls, the film can be moved, and the view 1,2,and 3 switches can be used to see the superposition of

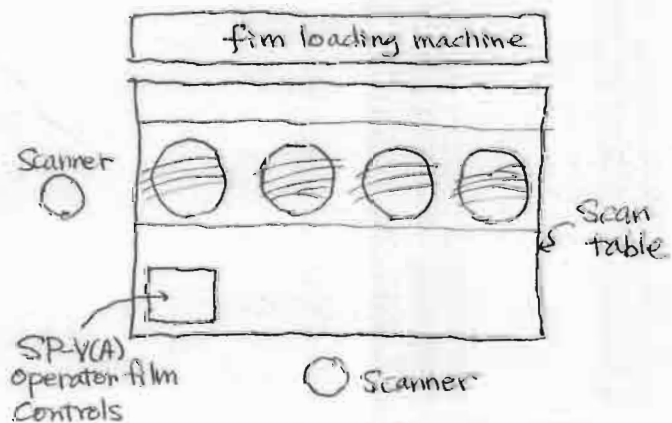


Figure 3

the views in which photos were taken from different directions. But, the frame number is correct only in the view 3. Now, we are ready to start scanning the films.

CALCULATIONS AND DATA REDUCTION - ANALYSIS

Having described the scanning procedure, I will now describe the results that were obtained from my 500 film scanning. All the raw data taken is contained at the end of this report, and the Table 1 below shows some numbers of events and the calculated value of the total number of incident K^- beam (discussed later).

kinds of events or number of beam	number of events
all decays (ΔN_D)	144
tau decays	8
interactions	137
elastic collisions ($\Delta N_{el.}$)	41
all interactions (ΔN_I)	178
total # of incident beam (N_0)	4860 ± 220

Table 1

1) Branching ratio

First of all, I determined the branching ratio of the ~~tau~~ decay from my data.

$$BR = \frac{\# \text{ of events } (K^- \rightarrow \pi^+ \pi^- \pi^-)}{\# \text{ of events } (K^- \rightarrow \text{all decay})} = \frac{8}{144} = 0.0556$$

Since the ratio of these two counts are not statistically independent, random error will be:

$$\sqrt{\frac{(8)(144)}{(144+8)^3}} = 1.81\% \quad \text{which is } 0.10\% \text{ of BR.}$$

Therefore, I conclude $BR = (5.56 \pm 0.10)\%$, and this value has only 2.5% discrepancy with the reference BR value.

2) Determination of the total number of incident K^- beam

I have to determine the total number of incident beam, N_0 , in 500 films before the further analysis. I estimate that number accurately enough by counting only 50 films randomly. Since the total number of incident beam in 50 films is $N_0 = 486$, using the Poisson statistics, the standard deviation is $(486)^{1/2} = 22.0$ (See Appendix 4). In order to get N_0 , I multiply these results by 10, and I conclude:

$$N_0 = 4860 \pm 220.$$

3) Correction for the cross sections

Before I start calculating the cross sections, I would like to calculate the correction value because I have the systematic errors included in my data. The major source of the systematic error is the difficulty in observing and identifying ~~a~~ small angle of K^-p scattering. To treat this situation, I assume that for the recoil length greater than 1 cm, I probably have a good scanning efficiency at all azimuth angles. To convert this to the proton momentum, I used the range-momentum graph (attached with raw data) found in Review of Particle Properties, and obtain $P_p = 143 \text{ MeV}/c$. Since in this case the momentum of incident K^- and the momentum of scattered K^- are almost the same ($P_K = 1.5 \text{ GeV}/c$), from the Figure 4, $P_K \theta \approx P_p$. Then I obtained $\theta = 0.0953 \text{ rad}$.

Now, to convert this small angle to the correction of the elastic cross section, I used the information that the differential cross section at small angle has been measured to be approximately $d\sigma/dt = 70 \text{ mb}/(\text{GeV}/c)^2$ where t is the square of the invariant 4-momentum transfer, and $t \approx (P\theta)^2$ at small angle. From the Figure 5,

$$t_{\min} \approx (P_K \theta_{\min})^2 = P_p^2 = 20450 (\text{MeV}/c)^2.$$

$$\Delta \sigma_{\text{el}} \approx (\Delta t) (d\sigma/dt) = 0.143 \text{ E-30 m}^2.$$

Therefore, I will add this value to the cross section values which will be calculated later in this report.

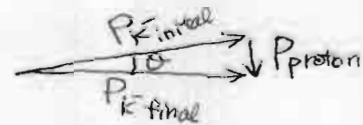


Figure 4

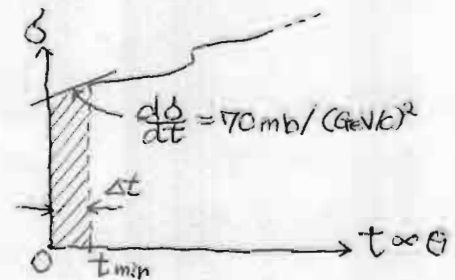


Figure 5

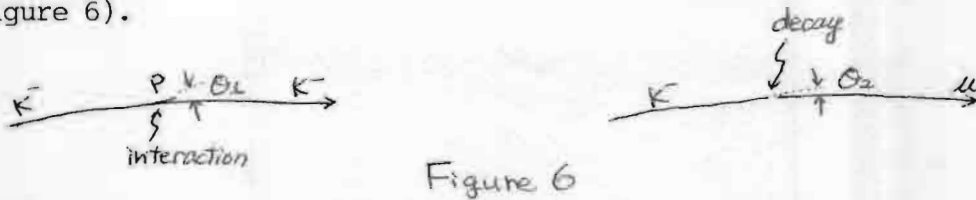
4) Correction of the systematic error for the number of decays

Before I calculate the K^- life time, I would like to correct the systematic error including in my data. The major source of this error is the fact that some $K^- \rightarrow \mu^- \bar{\nu}$ decays are missed since the mass of $\bar{\nu}$ particle is zero and these decays occur with nearly zero degree to the incident beam if the momentum change is small. Other 1 prong decays are involved by π^0 particle and its mass is sufficiently enough to reduce the momentum of the emerged particle so that the decay angles are enough to be detected. In the case of $K^- \rightarrow \mu^- \bar{\nu}$ decay, the neutrino momentum is:

$$P_{\bar{\nu}} = \frac{m_K^2 c^4 - m_{\mu}^2 c^4}{2(E_K c + P_K c)} \approx 37.8 \text{ MeV}/c \quad (\text{See derivation in Appendix 5})$$

Then the momentum of muon is $P_{\mu} = 1538 \text{ MeV}/c$, which corresponds to the nearly maximum momentum of the muon in the relativistic momentum diagram in the Appendix 6. From this diagram, I conclude that although the decay angle in general is large enough to see, when the decay angle $\theta = 0^\circ$, the decay is hard to detect.

Now, considering the ability of our eyes, I estimate that the minimum decay angle at which good scanning efficiency can be realized is approximately equal to the small angle of deflection of the kaon when the proton-recoil become invisibly small, which I discussed before. (Figure 6).



That is, $\theta_1 = \theta_2 = 0.0953$ rad. Then, since the kaon is spinless, its decay is isotropic in the center of mass frame, and we can approximate at small angles by $\theta = \theta^*/2$, where θ is the angle in lab frame and θ^* is that of the center of mass. It leads that:

$$\theta^* = 2\theta = 0.191 \text{ rad and}$$

$$\frac{0.191 \text{ rad}}{2\pi \text{ rad}} = 0.0303.$$

Thus, I can estimate that the fraction of kaon decays of 1 prong which were missed as a result of invisibly small kinks is 6.06%. (I multiply by two because θ^* is the angle above the incident beam line, and I need to add the angle below the incident line, too.) Now, from Table 1, the number of all decays is $\Delta N_D = 144$, and we know from the reference that the probability of $K^- \rightarrow \mu^- \gamma$ decay, ΔN_{μ} , is 50% of all decays, so ΔN_{μ} before considering the systematic error is 72. Then, I have the following equation:

$$\Delta N_{\mu} + (0.0606) \Delta N_{\mu, \text{corrected}} = \Delta N_{\mu, \text{corrected}}.$$

Then, $\Delta N_{\mu, \text{corrected}} = 77$. So, the number of all decays corrected is $\Delta N_{D, \text{corrected}} = 144 - 72 + 77 = 149$.

Although these discussions of systematic errors are non-inclusive, the major sources of errors are included, so I assume that the systematic errors will be nearly eliminated if I consider these corrections.

5) Calculation of the K^- life time

Considering the above discussions of the systematic errors, now I will calculate the life time τ using the equation below.

$$\frac{\Delta N_0}{\Delta x} = \frac{1}{\beta c \tau} \left(N_0 - \frac{\Delta N_{\mu} + \Delta N_D}{2} \right)$$

where now $N_0 = 4860 \pm 220$ (statistical error), $\Delta N_D = 149$, and $\Delta x = 0.2894 \text{ m}$.

Then, I obtained:

$$\tau = (1.04 \pm 0.05) \text{ E-8 sec.}$$

From the reference value $\tau_{\text{ref}} = 1.22 \text{ E-8 sec}$, discrepancy is 14.7%.

This % value is not small, and it suggests me that there are other

systematic or statistical errors involving. The one possibility that I remind now is the systematic error when I counted N_0 . There was a difficulty of distinguishing the parallel incident beam and un-paralleled beam. That is, sometimes I might include beams which do not have 1.5 GeV/c, such as the K^- beam that collided to proton before entering the fiducial volume.

Here, it is interesting that since the life time of K^- meson, τ , is extremely short, in general it is not feasible to measure it at rest. However, if K^- meson has a velocity which is close to the velocity of light (in my case, $\gamma = 1.39$ and $\beta = 0.950$), the pass it takes is measurable length for us, and it allows us to measure the life time.

6) Calculation of the cross sections

Next, I will calculate the elastic cross section σ_{el} and total cross section σ_t , using the equation below.

$$\frac{\Delta N_t}{\Delta x} = \frac{N_0 \sigma_p}{A} \left(N_0 - \frac{\Delta N_t + \Delta N_0}{2} \right)$$

Then, I obtained $\sigma_{el} = (0.81 \pm 0.04) \text{E-30m}^2$ and $\sigma_t = (3.47 \pm 0.16) \text{E-30m}^2$.

Adding $\Delta \sigma_{el}$ calculated before,

$$\sigma_{el} = (0.82 \pm 0.04) \text{E-30m}^2.$$

$$\sigma_t = (3.51 \pm 0.16) \text{E-30m}^2.$$

From the graph of the cross section vs. laboratory K^- beam momentum (attached at the back of this report) in the Review of Particle Properties, I read the reference values as:

$$\sigma_{t, \text{ref}} = 3.30 \text{E-30m}^2.$$

$$\sigma_{el, \text{ref}} = 0.85 \text{E-30m}^2.$$

Then, the discrepancy tests show that the % errors of my results are 6.4% and 3.5% respectively.

7) Calculation of the proton's effective radius

Based on my measured total cross section, I can calculate the proton's effective radius as follows:

Assuming the density of proton itself and the density of K^- meson are roughly

$$\text{equal, } \frac{\text{mass}}{\text{Volume}} \propto \frac{m_K}{R_K^3} = \frac{m_p}{R_p^3} \quad \therefore R_p = \left(\frac{m_p}{m_K} \right)^{\frac{1}{3}} R_K$$

But, from the Figure 7, $R_K = R_{\text{geo}} - R_p$.

And from my result, I set $\sigma_{\text{total}} \approx \sigma_{\text{geo}} = \pi R_{\text{geo}}^2$.

(This is reasonable since from Fraunfelder,

$\sigma_{\text{geometrical}} = 3 \text{fm}^2$) Combining these equations, the proton's radius will be:

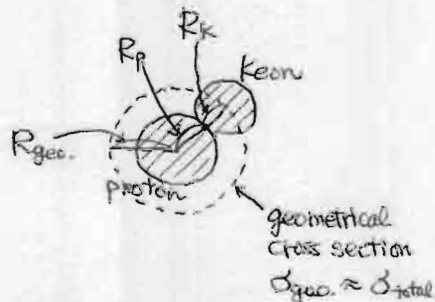


Figure 7

$$R_p \approx \frac{\left(\frac{m_p}{m_K}\right)^{\frac{1}{3}} \sqrt{\frac{8}{\pi}}}{1 + \left(\frac{m_p}{m_K}\right)^{\frac{1}{3}}} = 5.85 \times 10^{-16} \text{ m.} \quad \text{then with correction, } R_p \approx (5.85 \pm 0.14) \times 10^{-16} \text{ m.}$$

8) Determination of the resonant particle


Now, it is interesting to discuss the determination of a single resonant particle which will be formed by the K^-p interaction. Using the theory of special relativity, if we consider this event from the center of mass frame (Figure 8), the

velocity of that frame is $\beta_{cm} =$
 $Pc/E = 0.596$ so that $\gamma = 1.25$. Since

$$E_{\text{initial}} = \gamma E_{\text{cm}}, \text{ where } E_{\text{initial}} = \sqrt{(P_K c)^2 + (m_K c^2)^2} + m_p c^2, \quad E_{\text{cm}} = 2020 \text{ MeV.}$$

But, because the resonant particle is at rest in the center of mass frame, this energy value is the same to the rest mass of the resonant particle. Thus, $m_{\text{resonant}} = 2020 \text{ MeV}/c^2$.

From the table of the elementary particle in Perkins (page 412), this resonant particle might be $\Sigma(2030)$ or $\Lambda(2100)$. To determine one from these candidates, I have to check the quantum numbers. The Table 2 below shows the quantum numbers associated to this event.



	K^-	p	\rightarrow	resonant	$\Sigma(2030)$	$\Lambda(2100)$
charge	-	+		neutral	neutral	neutral
lepton	0	0		0	0	0
baryon	0	1		1	1	1
strangeness	-1	0		-1	-1	-1
isospin I	1/2	1/2		0, 1	1	0
I_3	-1/2	1/2		0	0	0

Table 2

From the table, isospin number makes me finally determine that this resonant particle is $\Sigma(2030)$ or Λ .

CONCLUSION

Well, this experiment has been particularly difficult since I had never studied particle physics before. Although my life time value has 14% discrepancy, I was surprised at my results of cross sections whose discrepancies are small. I think that my results will be improved if I carefully count the number of incident beam N_0 which momentum is 1.5 GeV/c only. Anyway, the experiment was very interesting as well as educational.

1) Modern Physics P.Tipler, 1978.

2) Introduction to High Energy Physics D.H.Perkins, Addison-Wesley, 1982.

3) Subatomic Physics H.Frauenfelder and E.M.Henry, Printice Hall, 1974.

4) Review of Particle Properties Rev.Modern Physics 56, 1984.

5) Alvares Group Scanning Training Memo in book form in Physics library.

APPENDIXCES

Appendix-1: Derivation of the effective number of meson averaged over the target length

From the equation, $N = N_0 \exp\left(\frac{-x}{\lambda_{\text{pion}}}\right) \exp\left(\frac{-x N_0 \sigma_p}{A}\right)$, if I set $a = \frac{1}{\lambda_{\text{pion}}}$ and $b = \frac{N_0 \sigma_p}{A}$, it will be $N = N_0 e^{-ax} e^{-bx}$. Then the effective number of K^- averaged over the target length is:

$$\begin{aligned} N &= N_0 \int_0^{\Delta x} \frac{e^{-(a+b)x}}{\Delta x} dx \\ &= \frac{N_0}{-(a+b)\Delta x} e^{-(a+b)x} \Big|_0^{\Delta x} \\ &= \frac{N_0}{\Delta x(a+b)} \left[e^{-(a+b)\Delta x} - 1 \right] \end{aligned}$$

If I take second order of expansion,

$$\begin{aligned} N &= \frac{N_0}{\Delta x(a+b)} \left[1 - 1 - (a+b)\Delta x + \frac{(a+b)^2(\Delta x)^2}{2} \right] \\ &= N_0 \left(1 - \frac{(a+b)\Delta x}{2} \right) \end{aligned}$$

On the other hand, I approximate $\frac{dN}{dx} = -(a+b)N$ to $\frac{\Delta N}{\Delta x} = -(a+b)N_0$ since $a+b \ll 1$, I have:

$$\frac{\Delta N_I}{\Delta x} = aN_0 \quad \text{and} \quad \frac{\Delta N_D}{\Delta x} = bN_0$$

So,

$$\Delta N_I = aN_0 \Delta x \quad \text{and} \quad \Delta N_D = bN_0 \Delta x$$

Therefore I obtained:

$$N = N_0 - \frac{\Delta N_I + \Delta N_D}{2}$$

By the way, this means that we approximate exponential curve to the straight curve as follows:



APPENDIX-2: More accurate way of the calculations for γ and δ

If we consider the decays in flight which could possibly interact if it does not decay, and vice versa, it means that ΔN_D and ΔN_I are dependent each other, and I think that this way of calculation is more accurate than the one introduced in my theory section.

Since $\frac{dN_D}{dx} = -a N(x)$ where $a = \frac{1}{\sigma \rho \epsilon x}$,

I set

$$\Delta N_D = -N_D = \int_0^{\Delta x} N(x) a dx$$

$$= a N_0 \int_0^{\Delta x} e^{-(a+b)x} dx$$

$$= \frac{a}{a+b} N_0 (1 - e^{-(a+b)\Delta x})$$

$$= \frac{a}{a+b} N_0 \left[(a+b)\Delta x - \frac{(a+b)^2 \Delta x^2}{2} + \dots \right]$$

Now, if I consider only first order term and neglect second,

$$\Delta N_D = a N_0 \Delta x.$$

This ΔN_D is independent on the factor of the interaction event, and I can't consider the number of decays which could possibly decay if they did not interact before.

So, I will take second order term also, then,

$$\Delta N_D = a N_0 \left[\Delta x - \frac{(a+b)\Delta x^2}{2} \right]$$

Similarly,

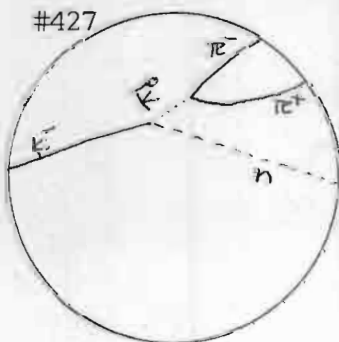
$$\Delta N_I = b N_0 \left[\Delta x - \frac{(a+b)\Delta x^2}{2} \right]$$

These two equations show that ΔN_D and ΔN_I are dependent each other, and if we solve for a and b from these equations, I believe that we can obtain more accurate values of γ and δ .

APPENDIX-3: Ten different kinds of events recorded (Roll number 5450)

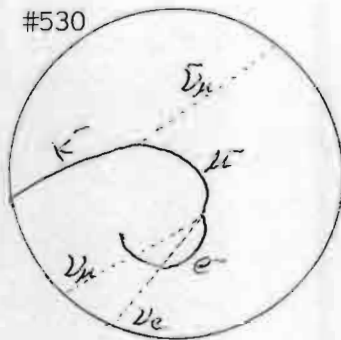
#427

Frame number 427



	$K^- + p \rightarrow n + \bar{K}^0$			
baryon	0	1	1	0
strangeness	-1	0	0	-1
	$\bar{K}^0 \rightarrow \pi^+ + \pi^-$			
baryon	0	0	0	0
lepton	0	0	0	0

#530



lepton

$$K^- \rightarrow \mu^- + \bar{\nu}_\mu$$

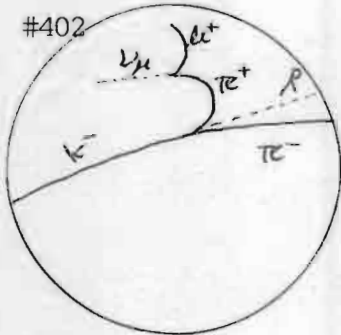
0	1	-1
---	---	----

lepton

$$\mu^- \rightarrow e^- + \bar{\nu}_e + \nu_\mu$$

1	1	-1	-1
---	---	----	----

#402



baryon

$$K^- + p \rightarrow \pi^+ + \pi^- + \Lambda^0$$

strangeness

0	1	0	0	1
-1	0	0	0	-1

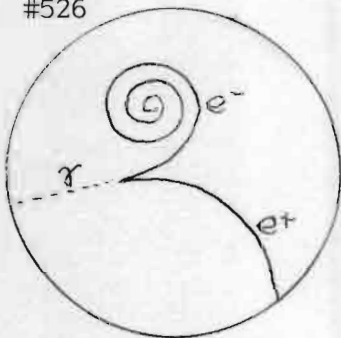
baryon

$$\pi^+ \rightarrow \mu^+ + \nu_\mu$$

lepton

0	0	0
0	-1	1

#526

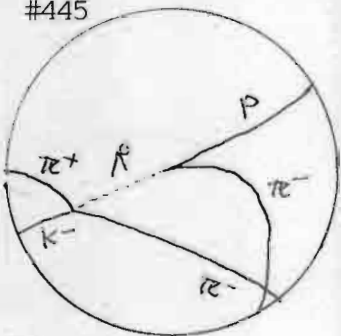


lepton

$$\gamma \rightarrow e^- + e^+$$

0	1	-1
---	---	----

#445

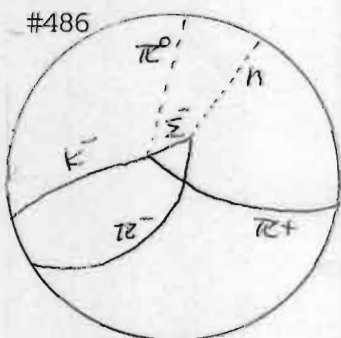


baryon

$$K^- + p \rightarrow \pi^+ + \pi^- + \pi^0$$

1	1	0
---	---	---

#486



baryon

strangeness

$$K^- + p \rightarrow \pi^- + \pi^+ + \Sigma^-$$

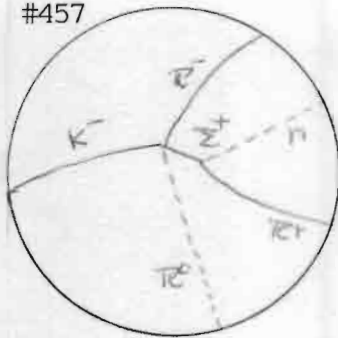
0	1	0	0	1
-1	0	0	0	-1

baryon

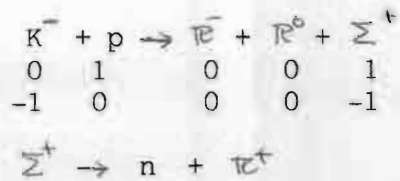
$$\Sigma^- \rightarrow n + \pi^-$$

1	1	0
---	---	---

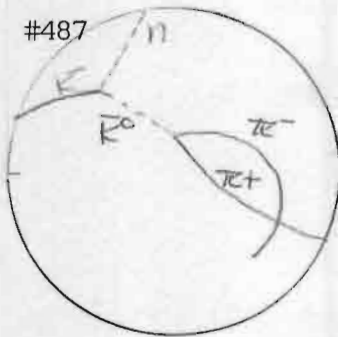
#457



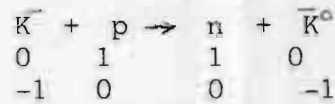
baryon
strangeness



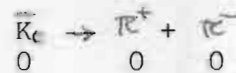
#487



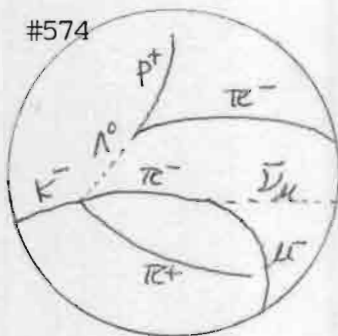
baryon
strangeness



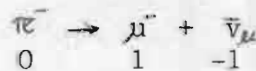
baryon



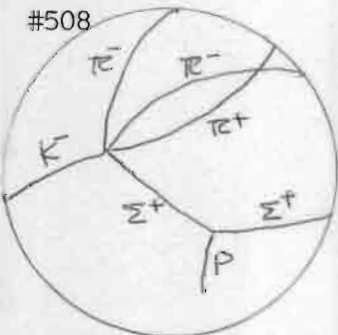
#574



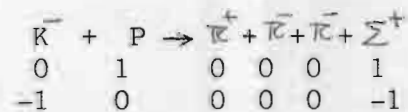
lepton



#508



baryon
strangeness



APPENDIX-4: Verification of the Poisson statistics in this case

The statistical error calculated by handy Poisson statistics way is varified by the ordinary way to calculate it.

Since $\sum_{i=1}^{50} N_0 = 486$, and $\bar{N} = 9.72$, standard deviation $= \sqrt{\frac{1}{49} \sum d_i^2}$ where $d_i = N_i - \bar{N}$ is 2.955. Then, $\sigma_{\bar{N}} = \frac{SP}{\sqrt{50}} = 0.42$

so that I obtain the average number of incident beam in one film:

$N_{1\text{film}} = 9.72 \pm 0.42$, so, for 500 films, $N_{500\text{films}} = 4860 \pm 210$ which is approximately same to the Poisson's way.

SLC 80

APPENDIX-5: Calculation of the neutrino and muon momentum

$$\begin{array}{ccc}
 \begin{array}{c} \text{K}^- \\ \rightarrow \\ \text{Initial} \end{array} &
 \begin{array}{c} \nu \quad \mu \\ \leftarrow \quad \rightarrow \\ \text{Final} \end{array} &
 \left\{ \begin{array}{l} m_K = 493.7 \text{ MeV}/c^2 \\ m_\mu = 105.7 \text{ MeV}/c^2 \\ m_\nu = 0 \\ P_K = 1.5 \text{ GeV}/c \end{array} \right.
 \end{array}$$

From the conservation of momentum,

$$\vec{P}_K = \vec{P}_\nu + \vec{P}_\mu$$

$$P_K = -P_\nu + P_\mu \quad \therefore P_\mu = P_K + P_\nu \quad \text{--- (1)}$$

From the conservation of energy,

$$E_K = E_\mu + E_\nu$$

$$E_K = \sqrt{(P_\mu c)^2 + m_\mu^2 c^4} + P_\nu c \quad \text{with (1),}$$

$$(E_K - P_\nu c)^2 = (P_K + P_\nu)^2 c^2 + m_\mu^2 c^4$$

solve for P_ν , then, we obtain:

$$P_\nu = \frac{m_\mu^2 c^4 - m_K^2 c^4}{2(E_K c + P_K c^2)} = 37.77 \text{ MeV}/c^2$$

$$\text{So, } P_\mu = 1538 \text{ MeV}/c^2$$

APPENDIX-6: Relativistic vector diagram for $K^- \rightarrow \bar{\nu} \mu$ decay

From the derivations of associated equations in the Reprint of Physics
111 Bubble chamber laboratory,

$$P_\mu^* \text{ of the center of mass frame} = \frac{(m_K c^2 + m_\mu c^2)(m_K c^2 - m_\mu c^2)}{2 m_K c^2} = 236 \text{ MeV}/c$$

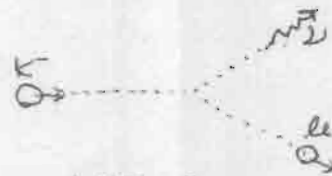
$$E_\mu = \frac{(m_K c^2)^2 + (m_\mu c^2)^2}{2(m_K c^2)} = 258 \text{ MeV}$$

$$\eta_0 = \frac{P_K}{M_K} = \frac{1.5 \text{ GeV}/c}{m_K c^2} = 3.038$$

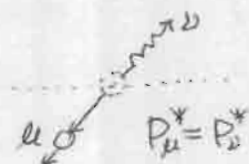
$$\gamma_0 = (\eta_0^2 + 1)^{\frac{1}{2}} = 3.19$$

$$\gamma_0 P^* = 754.4 \text{ MeV}/c$$

$$\eta_0 E_\mu = 783.8 \text{ MeV}$$

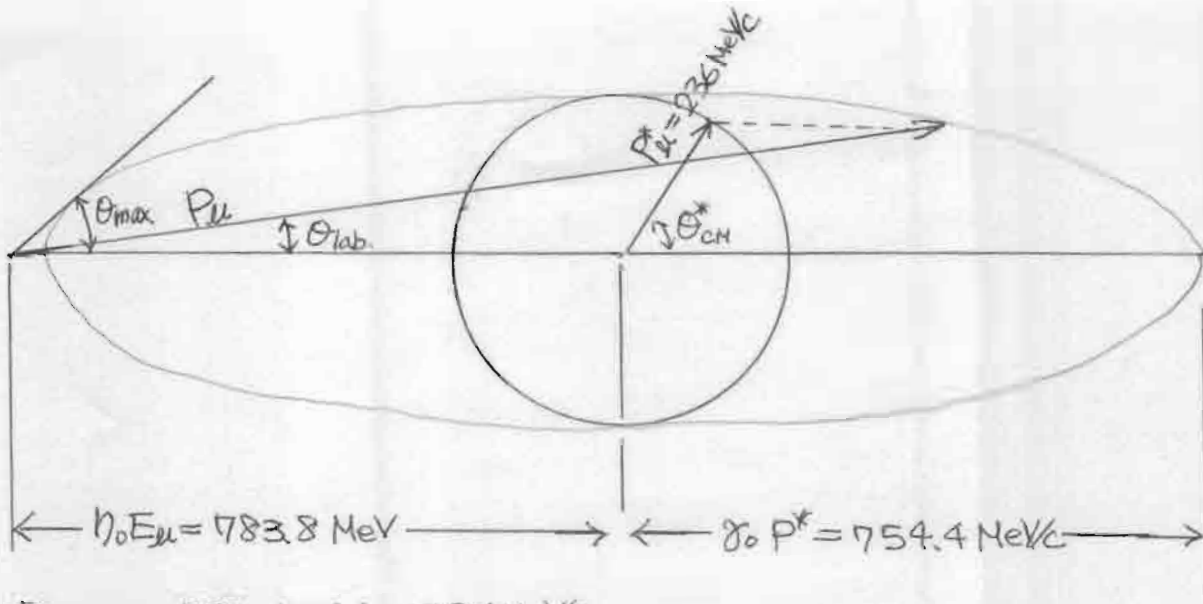


LAB frame



CM frame

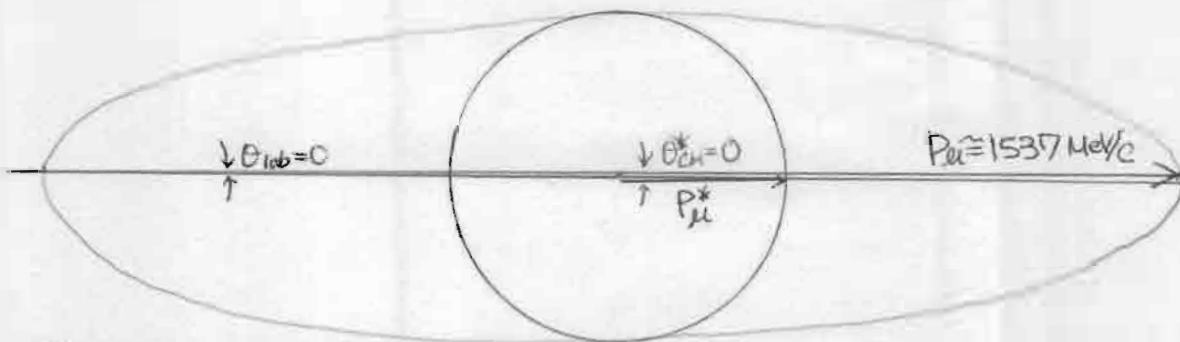
From the values above, we have the diagram as follows.



$$P_{\mu \text{ minimum}} = 783 - 754.4 = 28.6 \text{ MeV/c.}$$

$$P_{\mu \text{ maximum}} = 783 + 754.4 = 1537 \text{ MeV/c.}$$

The diagram below shows when $P_{\mu} \cong 1537 \text{ MeV/c.}$



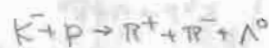
Obviously, $\theta_{\text{lab}} = \theta_{\text{CM}}^* \cong 0^\circ$.

So, the decay is hard to detect in this case.

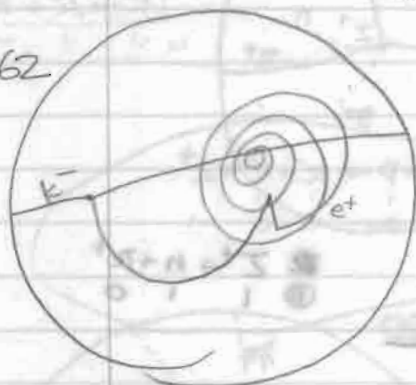
私達の向ひの

機舎と

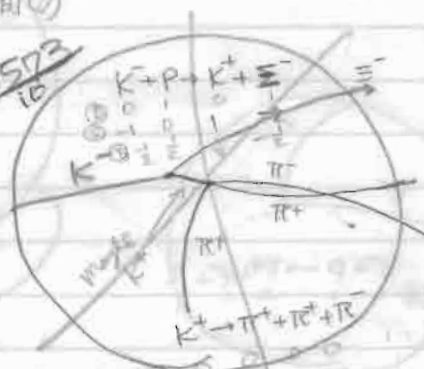
「新刊のまじり」



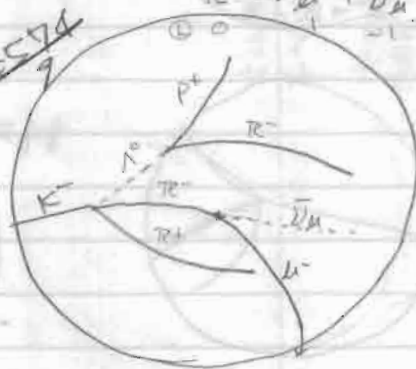
#562



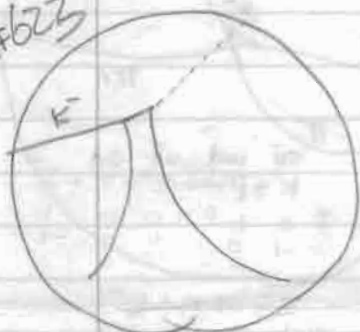
#573
10



~~#574~~
9



#623



#645



675



App-3

#427
5

$K + p \rightarrow n + \bar{K}$
 $\bar{K} \rightarrow \pi^+ + \pi^-$

$K + p \rightarrow \gamma + r$
 $\gamma \rightarrow e^+ + e^-$
 $K + p \rightarrow \bar{K} + n$
 $\bar{K} \rightarrow \pi^+ + \pi^-$

#432

$K \rightarrow \pi + \bar{\pi}$

#430

#438

$K + p \rightarrow \pi + \bar{\pi} + n$

#457
7

$K + p \rightarrow \pi + \bar{\pi} + n$

$K \rightarrow \mu + \bar{\nu}_\mu$

#402
2

$K + p \rightarrow \pi + \bar{\pi} + n$

#445
4

$K + p \rightarrow \pi + \bar{\pi} + n$

#480
6

$K + p \rightarrow \pi + \bar{\pi} + n$

#487
8

$K + p \rightarrow \pi + \bar{\pi} + n$

#508
10

$K + p \rightarrow \pi + \bar{\pi} + n$

#510

#511

#526
3

$\gamma \rightarrow e^+ + e^-$

#520
2

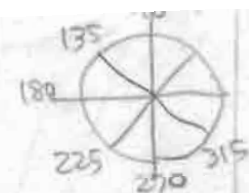
$K \rightarrow \mu + \bar{\nu}_\mu$

#550

$K \rightarrow \mu + \bar{\nu}_\mu$
 $\mu \rightarrow e + \bar{\nu}_e + \nu_\mu$



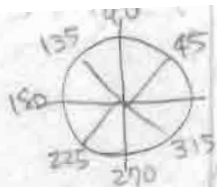
Frame	loc.	coll	int	decay	7	#	Δx
893	0.8 260			1p			0.8cm
894	0.7 260		91	1p			3.5cm
895	0.8 270		91	1p		11	1.4cm
	0.2 170	2p	91				19.7cm
896	0.6 160	2p	91				21.2cm
897 NO	0.4		91				
898	0.4 180			1p	93		12.6cm
899 900	0.8 270	2p			95		1.3cm
901	0.2 90			1p			23.5cm
902	0.9 290			1p			0.4cm
	0.3 180		91	1p			17.3cm
903 904	0.6 270		OP				2.5cm
	0.5 270	2p	91				6.3cm
905	0.3 180		91	1p		9	16.4cm



858	Frame	loc.	coll.	int	decay	n	#	dx
	859	0.3 150		2P				21.6cm
		0.8 210			1P			1.3cm
		0.5 300			1P			6.1cm
		0.4 300			1P			8.4cm
	860	0.9 230			1P			3.3cm
		0.7 140			1P			25.8cm
		0.6 260	2P					6.0cm
861	862	0.4 100	2P					29.1cm
	863	0.8 250				7		3.1cm
	864	0.6 100		0P				28.8cm
	865	0.6 140			1P		11	23.1cm
	866	0.3 290			1P			11.0cm
867	870	0.2 230			1P			14.1cm
868	871	0.8 250			1P			4.4cm
869	872	0.8 190				7		20.5cm
	873	0.4 140		2P				23.5cm
	874	0.7 140	2P					25.2cm
		0.8 270		2P				1.1cm
	875	0.7 230			1P		14	6.7cm
876	878	0.3 240			1P			10.6cm
877	879	0.4 140		4P				24.1cm
	880	0.2 190			1P			20.9cm
	881	0.8 280		0P+V				2.8cm
	882	0.2 180			1P			17.4cm
883	884	0.4 260		0P+V				8.5cm
		0.7 220		2P				9.9cm
		0.8 190		2P				21.1cm
	885	0.1 120			1P		10	19.4cm
886	887	0.5 190		2P				19.4cm
		0.5 190			1P			19.2 cm
	888	0.7 290	2P					1.4cm
889	890	0.9 250			1P			0.3cm
		0.4 60		2P				27.6cm



From	loc. #	coll:	int	decay	T	#	dx
8003	0.6 210	2P				14	11.9cm
8006	0.6 220		2P				12.7cm
808	0.5 190			1P			15.6cm
	0.5 260		2P				7.4cm
810	0.6 190			1P		13	19.0cm
815	0.8 250	2P					2.2cm
817	0.5 230		4P				11.1cm
	0.4 90		2P				24.8cm
818	0.6 100		2P				28.8cm
819	0.3 240			1P			11.8cm
	0.6 220		0P+V				10.4cm
821	center			1P			16.9cm
	0.1 140		2P				19.4cm
822	0.6 140			1P			25.5cm
	0.6 220			1P			10.7cm
823	0.5 220			1P			12.7cm
825 NO						12	
827	0.7 180			1P			17.8cm
	0.6 130			1P			26.9cm
828	0.8 260		2P+V				1.5cm
	0.4 230		2P				11.8cm
832	0.9 220		2P+V				3.5cm
833	0.6 180		2P				19.7cm
835 NO							
836	0.6 210		2P			10	12.1cm
837	0.3 290			1P			10.2cm
839	0.5 190			1P			14.9cm
844	center		2P				16.7cm
845 NO						7	
846	0.8 260			1P			1.6cm
849	0.5 240			1P			7.7cm
853	0.6 120		2P				29.4cm
857	0.3 100		2P			10	24.1cm



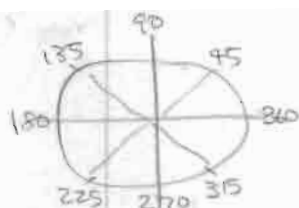
From #	loc.	Colli.	int.	delay	~	#	ΔX
753	0.8 250			1P			3.2cm
754	0.7 300			1P			3.0cm
755 NO						12	
756 NO							
758	0.8 260			1P			0.5cm
760	0.3 250			1P			10.9cm
761	0.2 170			1P			18.9cm
762	0.5 270			1P			6.2cm
765 NO						7	
766	0.6 260			1P			2.8cm
768	0.7 230		2P				5.0cm
	0.4 150			1P			22.7cm
769	0.4 180		2P				17.2cm
770	0.7 230		4P				9.1cm
774	0.8 270			1P			1.1cm
775 NO						10	
780	0.2 110		2P+V				21.6cm
	0.4 110		2P				26.4cm
782	0.2 270		2P				13.0cm
	0.5 230			1P			10.1cm
784	0.7 260		0P				3.6cm
	0.5 290	2P					6.2cm
785 NO						6	
786	0.1 180		2P				17.5cm
	0.5 170		2P				19.5cm
789	0.5 90	2P					26.9cm
790	0.8 140			1P			27.9cm
792	0.3 140		2P				22.7cm
795	0.3 190		2P			16.	15.9cm
797	0.5 300		0P				8.1cm
798	0.6 220			1P			17.6cm
800	0.6 170			1P			20.6cm
	0.8 280			1P			0.7cm

Frame	loc.	calli	int.	decay	T	#	ΔX
697	0.4 250			1P			8.4cm
	0.5 130	2P					22.9cm
	0.7 230			1P			9.9cm
698	0.7 290			1P			2.5cm
701	0.4 250			1P			10.9cm
702	0.3 250		2P				9.4cm
703	0.3 120			1P			21.4cm
	0.4 120		2P				24.1cm
704	0.4 260			1P			2.7cm
	0.8 120	2P					28.8cm
705 NO						11	#
706	center	2P					17.1cm
708	0.3 90			1P			24.9cm
709	0.9 250			1P			3.7cm
	0.7 250		2P				7.6cm
	0.6 130			1P			22.7cm
	0.5 110		2P				25.9cm
710	0.8 280			1P			0.6cm
712	0.6 110			1P			28.5cm
713	0.8 290		2P				0.2cm
715 NO						12	
717	0.7 200	2P					12.5cm
722	0.3 290			1P			13.0cm
724	0.6 300			1P			4.1cm
	0.6 290			1P			4.6cm
725	0.4 320		2P			14	10.1cm
731	0.6 240			1P			8.4cm
739	0.4 320		2P				10.6cm
742	0.9 240		2P				1.1cm
743	0.5 240			1P			8.5cm
745 NO							

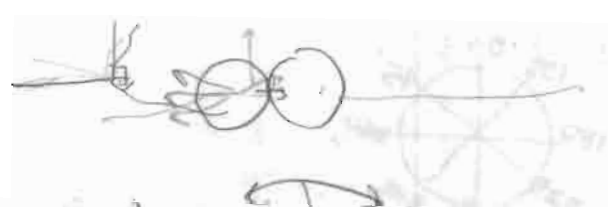
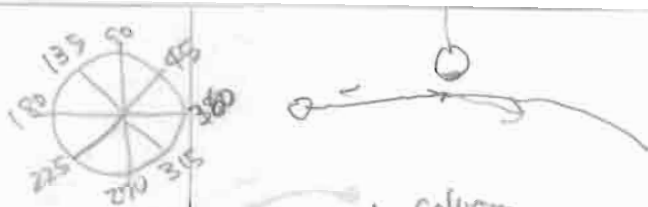
Frame#	location	coll:	int	decay	τ	Δx	# beam
668	0.4 100	2P				25.7cm	
	0.8 140			1P	→	27.1cm	
669	0.7 150			1P	→	24.9cm	
670	0.8 260	2P				2.4cm	
671	0.9 250	2P				0.6cm	
673	0.4 150				τ →	19.9cm	
	0.6 100	2P				29.0cm	
674	0.6 240			1P	→	6.0cm	
	0.1 90°			1P	→	21.7cm	
675	0.8 240		2P			6.1cm	12
677	0.3 190°			1P	→	15.0cm	
678	0.7 240°			1P	→	7.6cm	
	0.6 240°		2P			9.0cm	
	0.7 270°		2P			4.4cm	
681	0.5 170°		2P			20.8cm	
	0.2 260°		2P			12.7cm	
682	0.6 240°	2P				7.3cm	
683	0.8 220°		2P			8.6cm	
685	0.9 250°			1P	→	2.7cm	10
686	0.3 260°		2P			10.7cm	
687	0.3 110°			1P	→	23.8cm	
688	0.7 240°	2P+decay				6.8cm	
	0.5 180°		2P			16.8cm	
689	0.2 170°	2P				18.8cm	
690	0.4 210°		2P			13.7cm	
691	0.1 170°			1P	→	18.1cm	
	0.8 250°			1P	→	4.4cm	
	0.6 230°		2P			8.7cm	
694	center		2P			13.9cm	
	0.5 240		2P			2.6cm	
	0.5 240				τ →	10.8cm	
695	0.6 230°		2P				



Frame#	location	Collision	int.	decay	γ	Δx	beam
601	0.6 220°			1p		10.3cm	
602 NO							
603 NO							
604 NO	0.4 230°			1p		9.0cm	10
605	0.8 240°		0p			3.9cm	
606	0.3 190°		2p			16.0cm	
607	0.2 100°	2p				21.6cm	
608, 609 NO							
610	0.5 190°		2p			15.1cm	
616	0.8 240	2p				3.8cm	
617	0.5 240		2p			7.4cm	
621	0.2 180	2p				16.9cm	
622	0.8 140			1p		26.0cm	
623	0.6 250°		2p			5.4cm	
627	0.7 310°		2p			1.7cm	
630	0.2 140°		2p			18.1cm	
631	0.8 160°	2p				22.8cm	
634	0.6 240°	2p				6.9cm	
635 NO							8
637	0.7 260°		4p			3.8cm	
642	0.4 100°	2p				25.1cm	
645 NO							
646	0.6 270			1p		2.3cm	
648	0.5 130°		2p			24.0cm	
649	0.5 160°		2p			20.6cm	
655 NO							9
660	0.5 120°			1p		26.3cm	
665	0.4 180°			1p		18.0cm	6
666	0.3 90°		2p			23.4cm	



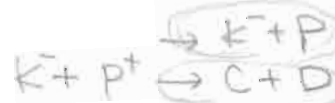
Framett	Location	Collision	int	decan	# of beam	ΔX
574 NO	0.6 280°		2P			3.3cm
575	0.6 280°		2P		13	3.3cm
576	0.5, 180°		OptV			15.8cm
577	0.6, 130°			1P		28.1cm
	0.5 170°		2P			17.8cm
	0.8 240°	2P				5.6cm
578	0.2 270°			1P		12.0cm
579	0.5 190°		2P			14.5cm
580	0.8 250°			1P		5.2cm
	0.4 220°		2P			13.7cm
581	0.7 260°		2P			2.6cm
582	0.9 240°			1P		1.1cm
583 NO						
584 NO						
585 NO					3	
586	0.9 230		OP			0.3cm
	0.8 230			1P		3.3cm
	0.2, 210			1P		14.3cm
587 NO						
588	0.7, 240			1P		6.2cm
589 NO						
590 NO						
591	0.8 260		2P			1.6cm
592 NO						
593	0.2, 180°	2P				16.8cm
594	0.5 250			1P		7.7cm
595 NO					9	
596	0.8 260			1P		1.0cm
	0.4 270°		2P			7.8cm
597	0.5 240		OP			8.1cm
598	0.4 230		2P			11.5cm
599	0.5 130°		OP			23.9cm
600	0.4 130°		2P			14.4cm
	0.6 260°		2P			5.1cm



Fract	location	Collision elast.	int.	decay	TT	Δx cm	# of beams
543 NO	0.6, 230°		2p			9.6	10.4cm
	0.8, 250°		2p				0.4cm
544	0.1, 190°			1p			19.2cm
545	0.9, 240°			1p			3.3cm
546 NO						12	
547 NO							
548 NO							
549 NO							
550	0.4, 180°	2p					18.2cm
551	0.9, 240°		2p			9.6	2.6cm
552 NO							
553 NO							
554 NO							
555 NO						4	
556 NO							
557	0.9, 140°			1p			27.3cm
	0.8, 140°	2p					27.5cm
558 NO							
559	0.5, 120°			1p			25.1cm
	0.6, 150°		2p				25.7cm
560 NO							
561 NO							
562	0.8, 250°		2p				2.2cm
563 NO							
564 NO						12	
565 NO							
566 NO							
567 NO							
568 NO							
569	0.4, 180°		0p				12.1cm
570 NO							
571	0.1, 80°		2p				20.7cm
572	0.6, 240°		2p				7.8cm
573			2p				



Frame#	location	elastic	int.	decay	γ	Δx cm	# of beam
511	0.4 130°	2p					24.4cm
	0.4 30°		2p				23.0cm
512	0.1 20°				γ		18.0cm
513 NO							
514 NO							
515 NO						6	
516 NO							
517	0.8 240°		2p + Vec				1.9cm
518 NO							4.6cm
519	0.6 260°	2p					4.6cm
520 NO	0.5 240°				γ		8.3cm
521	0.5 240°				γ		8.3cm
522 NO							
523 NO							
524	0.4 110°		0p				24.5cm
525	0.5 130°		4p			11	27.2cm
526 NO							
527	0.4 270°			1p			8.4cm
528	0.8 260°		2p				0.5cm
529 NO							
530	0.6 230°			1p			5.5cm
	0.5 190°		2p				16.3cm
531 NO							
532	0.5 230°		2p				8.6cm
	0.7 100°						28.3cm
533 NO							
534	0.4 190°		2p				16.1cm
535 NO						6	
536	0.2 140°			1p			19.4cm
537	0.8 270°			1p			0.5cm
538	0.7 190°		2p				13.5cm
539 NO							
540 NO							
541	0.7 210°						11.5cm



Frame#	location	elastic int.	interaction	decay	Tdecay	(cm) ΔX	# of beams
481						12.9cm	
482	0.7 190°			1p		4.6cm	20
483	0.4 260°		2p			9.3cm	(0.1) 20
484 NO							20
485 NO							12
486 NO							12
487	0.9 240°		Op+Vec			4.2cm	(0.1) 20
488 NO							20
489	0.8 140°				τ -decay	27.1cm	12
490 NO							20
491 NO							20
492 NO							20
493 NO							20
494	0.3 260°		Op			11.2cm	20
	0.4 200°			1p		17.5cm	5
495 NO							20
496	0.6 250°			1p		5.3cm	20
497	0.7 280°		Op			2.6cm	20
498 NO							20
499 NO							20
500 NO							20
501 NO							20
502	0.8 240°		Op			4.4cm	20
503	0.4 130°		2p			26.2cm	20
504 NO							20
505 NO							6
506 NO							20
507	0.7 200°			1p		14.7cm	20
	0.7 140°		2p			26.6cm	20
	0.7 270°		4p			1.1cm	20
508	0.8 240°			1p		4.9cm	20
509 NO							20
510	0.5 170°		2p			18.8cm	20



Frame#	Location	Elastic int.	Interaction	Decay	γ decay	Δx	# of beams
452	0.6, 230°	2P				54.1cm	10
453 (NO)				90			10
454	0.5, 100°			1P		29.3cm	04 P9P
455	0.7 230°	2P				8.2cm	04 29P
	0.7, 240°			1P		3.0cm	11 tracks
456 (NO)				90			90
457	0.3, 180°	2P				19.2cm	04 83P
458 NO							90
459	0.8 270°	2P				0.3cm	04 01P
460	0.2 100°			1P		23.8cm	04 19P
461 NO							04 29P
462	0.7 180°	2P				17.0cm	04 50P
463 NO				90			50
464 NO							
465 NO							10 tracks
466 NO			91				90
467 NO				90			90
468	0.7, 230°			1P		7.8cm	04 91P
469 NO							04 91P
470	0.4 230°			1P		12.4cm	04 002
471 NO							04 102
472	0.9, 240°			1P		1.9cm	002
473	0.7 220°	OP		90		10.8cm	04 902
474 NO							04 902
475 NO							10 202
476 NO							04 202
477 NO			91				902
478	0.8 260°	2P		90		1.4cm	
479 NO				90			902
480	0.8 230°	OP				8.0cm	
	0.3 180°					16.1cm	04 902
481	0.5 230°			1P		12.9cm	012



LEPT all

	location	elastic int.	interaction	decay	Tdecay	ΔX	# of beam
425	0.4, 130°		2 prong				23.3cm
425 (no)							
427	0.5, 230°		0 prong				7.2cm
	0.4, 180°	2 prong					16.1cm
428 (no)							
429	0.6, 120°		2 prong				25.2cm
	0.5, 190°			1 prong			14.2cm
							23.6cm
430	0.3, 110°		4 prong				
431							
432	0.3, 180°	2 prong	2 prong				17.8cm
433	0.3, 210°			1 prong			14.5cm
	0.3, 130°	2 prong					22.3cm
434	0.4, 150°			1 prong			21.4cm
	0.6, 140°		0 prong				22.9cm
	0.7, 130°	2 prong					26.2cm
435 no						8	26.2cm
436	0.2, 260°	2 prong					13.2cm
	2.4, 120°		2 prong				26.0cm
437 (no)							
438	0.5, 130°		2 prong				24.0cm
	0.6, 140°			1 prong			23.4cm
439	0.5, 170°			1 prong			21.4cm
440 no							
441 no							
442	0.3, 190°			1 prong			17.4cm
443	0.4, 250°			4 prong			17.4cm
444	0.8, 260°		2 prong				3.9cm
	0.9, 90°			1 prong			28.1cm
445	1.0, 270°		2 prong				0.4cm
	0.9, 280°			1 prong		11	2.1cm
446 (no)	0.3, 280°		0 prong				10.9cm
447	0.4, 220°		0 prong				12.8cm
448 (no)							
449 (no)							
450	0.2, 230°		2 prong				13.4cm



elastic int.
interactions
decays
3 prongs (with use)

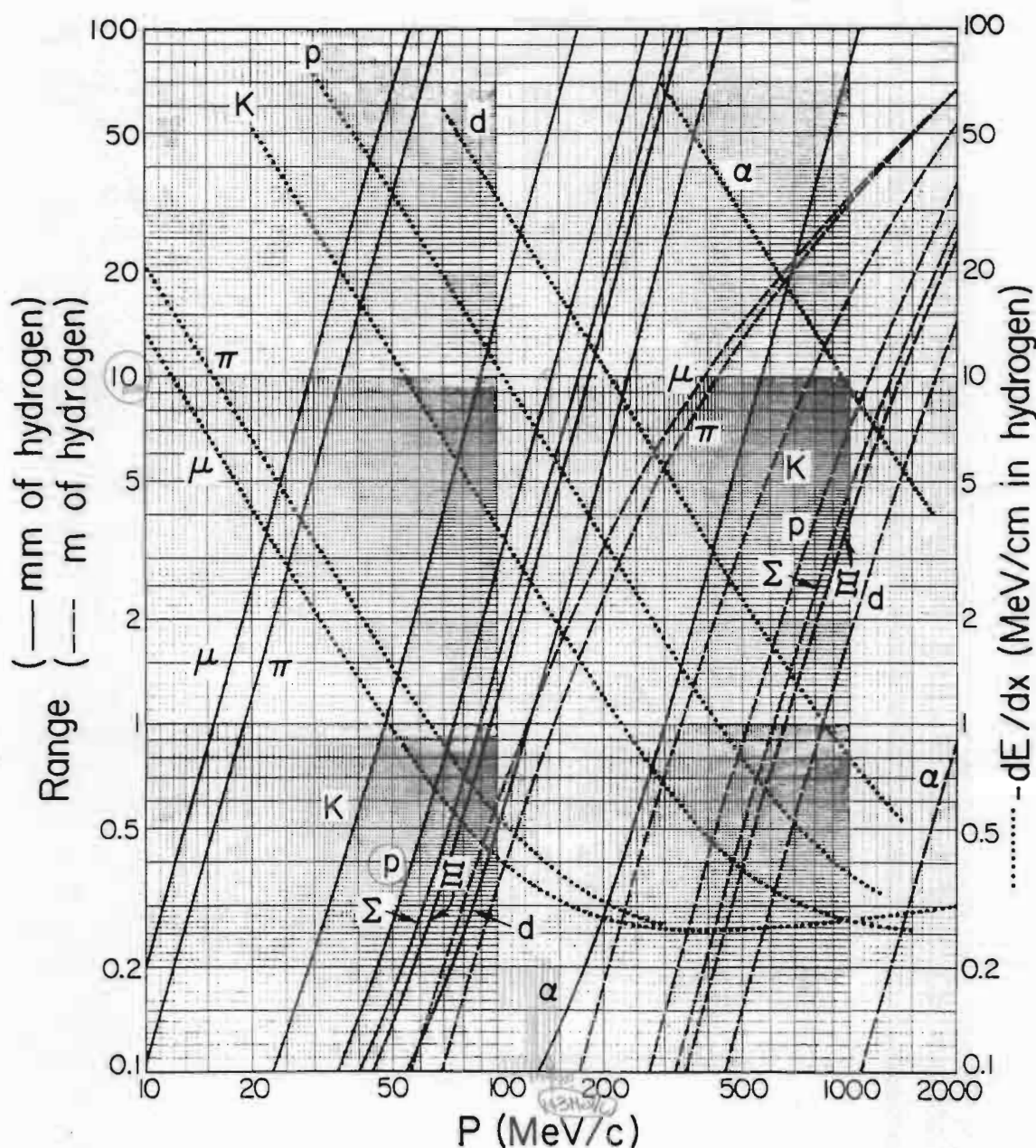


roll# 5450

Frame# (No.)	(cm, °) rough location	elastic int. 5 prng	interaction	decay	τ decay	(cm) ΔX	# of Beams
1 0395							
2 0396	0.8, 290°		4 prong			8.9cm	
3 0397							
4 0398							
5 0399	0.8, 260°	2 prng	2 prng			2.1cm	
6 0400	0.8, 230°	2 prng	0 prng			6.2cm	
7 0401	0.5, 240°			1 prng	→	11.5cm	
8 0402	0.6, 180°		2 prng			21.3cm	
9 0403						25.0cm	
10 0404	0.5, 120°			1 prng			
11 0405	0.6, 120°			1 prng	→	22.5cm	13
12 0406							
13 0407							
14 0408	0.5, 270°			1 prng	→	6.8cm	
15 0409	0.3, 180°			1 prng	→	18.5cm	
16 0410	0.7, 140°		0 prng			28.4cm	
17 0411	0.2, 100°				→	23.3cm	
18 0412	0.5, 240°		4 prng			12.3cm	
19 0413							
20 0414	0.8, 270°			1 prng	→	1.0cm	10
21 0415	0.4, 190°	2 prng	2 prng			19.5cm	
22 0416							
23 0417							
24 0418	0.7, 250°			1 prng	→	2.7cm	
25 0419	0.8, 230°			1 prng	→	4.5cm	
26 0420	0.7, 230°			1 prng	→	6.1cm	
27 0421							
28 0422							
29 0423	0.3, 180°			1 prng	→	19.7cm	
30 0424	0.7, 140°	2 prng	2 prng			26.9cm	5

PARTICLE DETECTORS, ABSORBERS, AND RANGES (Cont'd)

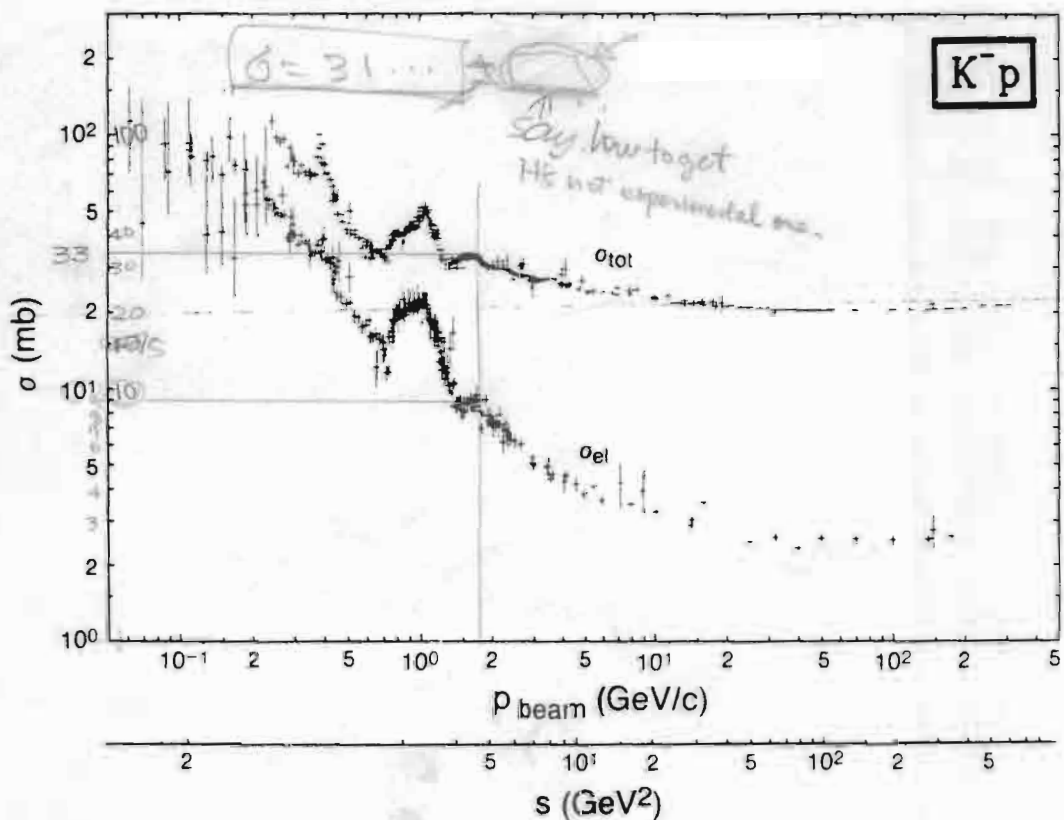
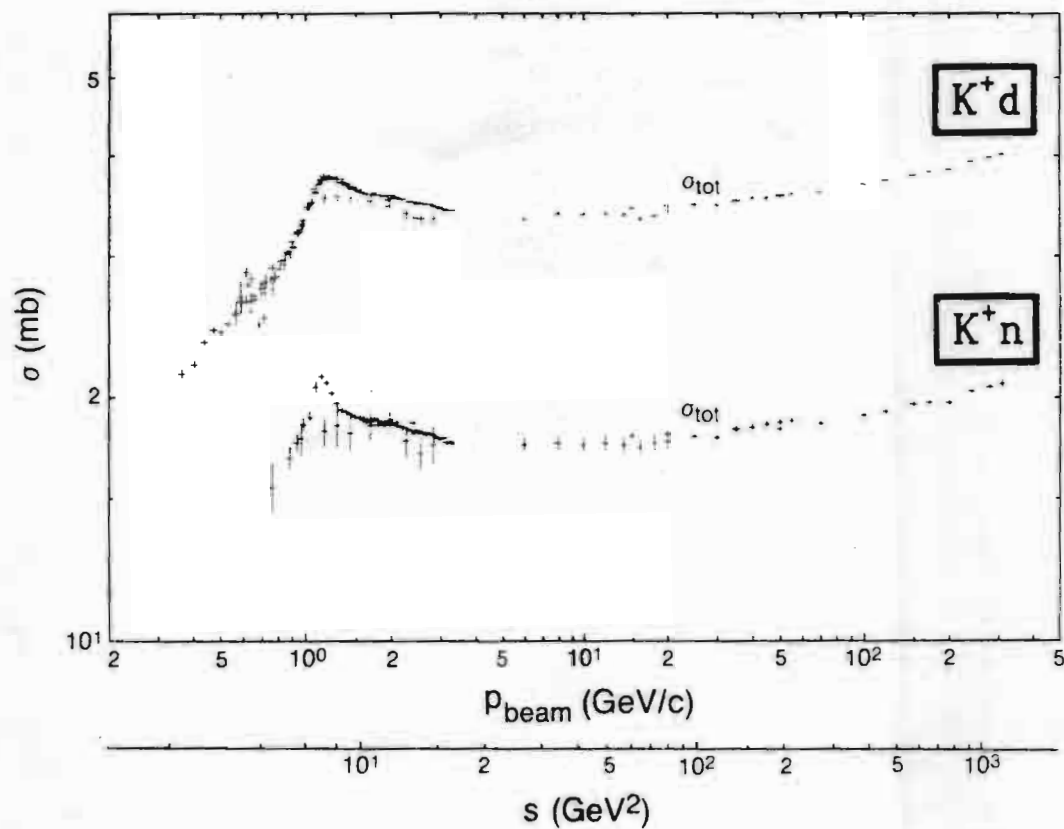
Mean Range and Energy Loss in Liquid Hydrogen



Range and energy loss in liquid hydrogen bubble chamber, based on Bethe-Bloch equation (Section C.1 above), using an average ionization potential for H_2 of $I = 20.0$ eV, which is an approximate average of the experimental result of Garbincius and Hyman [Phys. Rev. A2, 1834 (1970)] and the theoretical result of Ford and Browne [Phys. Rev. A7, 418 (1973)]. Bubble chamber conditions are chosen to be those of Garbincius and Hyman: parahydrogen of density $= 0.0625$ g/cm³ (note: range $\propto 1/\text{density}$), with vapor-pressure 60.8 lb/in² (absolute) and temperature 26.2°K. The functional dependence of the Bethe-Bloch equation is not experimentally verified to better than about $\pm 1\%$ over large momentum ranges. It should be noted that the number of bubbles per cm of a track in a bubble chamber is nearly proportional to $1/\beta^2$, not dE/dx . For the linear portions of the range curves, $R \propto p^{3.6}$. *Scaling law for particles of other mass or charge (except electrons):* for a given medium, the range R_b of any beam particle with mass M_b , charge z_b , and momentum p_b is given in terms of the range R_a of any other particle with mass M_a , charge z_a , and momentum $p_a = p_b M_a/M_b$ (i.e., having the same velocity) by the expression:

$$R_b(M_b, z_b, p_b) = \left[\frac{M_b/M_a}{z_b^2/z_a^2} \right] R_a(M_a, z_a, p_a = p_b M_a/M_b).$$

PLOTS OF CROSS SECTIONS AND RELATED QUANTITIES (Cont'd)



Hadronic total and elastic cross sections vs. laboratory beam momentum p_{beam} and center-of-mass energy squared s . Figures courtesy V. Flaminio, W.G. Moorhead, D.R.O. Morrison, and N. Rivoire, CERN.